Article

Designing PbSe Nanowires and Nanorings through Oriented Attachment of Nanoparticles

Kyung-Sang Cho, Dmitri V. Talapin, Wolfgang Gaschler, and Christopher B. Murray

J. Am. Chem. Soc., **2005**, 127 (19), 7140-7147• DOI: 10.1021/ja050107s • Publication Date (Web): 23 April 2005

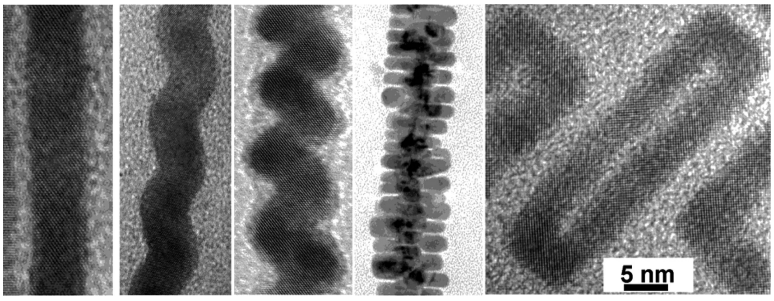

J|A|C|S
ARTICLES
Published on Web 04/23/2005

Designing PbSe Nanowires and Nanorings through Oriented Attachment of Nanoparticles

Kyung-Sang Cho,[†,‡] Dmitri V. Talapin,*[,†] Wolfgang Gaschler,[†,‡] and Christopher B. Murray*[,†]

Contribution from the Nanoscale Materials and Devices Group, IBM T. J. Watson Research Center, Yorktown Heights, New York 10598, and Advanced Materials Research Institute (AMRI), The University of New Orleans, New Orleans, Louisiana 70148

Received January 7, 2005; E-mail: dmitrit@us.ibm.com (D.V.T.); cbmurray@us.ibm.com (C.B.M.)

Abstract: Single-crystal PbSe nanowires are synthesized in solution through oriented attachment of nanocrystal building blocks. Reaction temperatures of 190−250 °C and multicomponent surfactant mixtures result in a nearly defect-free crystal lattice and high uniformity of nanowire diameter along the entire length. The wires' dimensions are tuned by tailoring reaction conditions in a range from ∼4 to ∼20 nm in diameter with wire lengths up to ∼30 μm. PbSe nanocrystals bind to each other on either {100}, {110}, or {111} faces, depending on the surfactant molecules present in the reaction solution. While PbSe nanocrystals have the centrosymmetric rocksalt lattice, they can lack central symmetry due to a noncentrosymmetric arrangement of Pb- and Se-terminated {111} facets and possess dipole driving one-dimensional oriented attachment of nanocrystals to form nanowires. In addition to straight nanowires, zigzag, helical, branched, and tapered nanowires as well as single-crystal nanorings can be controllably prepared in one-pot reactions by careful adjustment of the reaction conditions.

Introduction

Semiconductor nanowires may one day be employed in high-performance field-effect transistors (FETs),[1,2] logic circuits,[3] nonvolatile memories,[4] and biosensors.[5] They are considered promising candidates to augment or even replace silicon planar technology, which is approaching fundamental scaling limits.[6]

Nanowire-based applications demand nanowires with controlled composition, diameter, length, and morphology. Various techniques, including vapor−liquid−solid (VLS) and solution−liquid−solid (SLS) phase catalytic growth,[7−10] templated growth inside nanopores,[11,12] deposition along steps in surfaces,[13] and oriented attachment of nanoparticles,[14−18] have been reported for the synthesis of semiconductor nanowires. The major challenge for synthesis is to provide a crystalline nanowire uniform in diameter along the entire nanowire length. To date, VLS and SLS methods have provided semiconductor nanowires best suited to a broad range of device applications.

In this work, we report the solution-based synthesis of crystalline PbSe nanowires by oriented attachment of collections of nanocrystals that attach and fuse along identical crystal faces forming oriented chains. We employ reaction temperatures of 190−250 °C to allow efficient annealing of crystalline defects, and we utilize surfactant mixtures to mediate growth and achieve nanowires uniform in diameter. The entire process of nanowire formation and growth is fast. Wires usually assemble within 1 min after the start of reaction. Our approach allows obtaining large quantities of high-quality, catalyst-free semiconductor nanowires. These nanowires can form stable colloidal dispersions and, therefore, are easy for solution-processing and device integration.

Nanowire synthesis through oriented attachment produces nanowires with control of wire dimensions and morphology. In addition to straight nanowires, zigzag, helical, branched, and tapered nanowires as well as single-crystal nanorings could all be prepared by adjustment of the reaction conditions. The

* Correspondence and requests for materials should be addressed to Dmitri V. Talapin and/or Christopher B. Murray.
† IBM T. J. Watson Research Center.
‡ University of New Orleans.

(1) Cui, Y.; Zhong, Z.; Wang, D.; Wang, W. U.; Lieber, C. M. *Nano Lett.* **2003**, *3*, 149−152.
(2) Duan, X.; Niu, C.; Sahi, V.; Chen, J.; Parce, J. W.; Empedocles, S.; Goldman, J. L. *Nature* **2003**, *425*, 274−278.
(3) Huang, Y.; Duan, X.; Cui, Y.; Lauhon, L. J.; Kim, K.-H.; Lieber, C. M. *Science* **2001**, *294*, 1313−1317.
(4) Duan, X.; Huang, Y.; Leiber, C. M. *Nano Lett.* **2002**, *2*, 487−490.
(5) Patolsky, F.; Zheng, G.; Hayden, O.; Lakadamyali, M.; Zhuang, X.; Lieber, C. M. *Proc. Natl. Acad. Sci. U.S.A.* **2004**, *101*, 14017−14022.
(6) International Technology Road Map for Semiconductors, 2003 edition (http://public.itrs.net/).
(7) Gudiksen, M. S.; Wang, J.; Lieber, C. M. *J. Phys. Chem. B* **2001**, *105*, 4062−4064.
(8) Law, M.; Goldberg, J.; Yang, P. *Annu. Rev. Mater. Res.* **2004**, *34*, 83−122.
(9) Trentler, T. J.; Hickman, K. M.; Goel, S. C.; Viano, A. M.; Gibbons, P. C.; Buhro, W. M. *Science* **1995**, *270*, 1791−1794.
(10) Holmes, J. D.; Johnston, K. P.; Doty, R. C.; Korgel, B. A. *Science* **2000**, *287*, 1471−1473.
(11) Wang, W.; Huang, Q.; Jia, F.; Zhu, J. *J. Appl. Phys.* **2004**, *96*, 615−618.
(12) Al-Mawlawi, D.; Liu, C. Z.; Moskovits, M. *J. Mater. Res.* **1994**, *9*, 1014−1018.
(13) Wang, Y.; Sibener, S. J. *J. Phys. Chem. B* **2002**, *106*, 12856−12859.
(14) Penn, R. L.; Banfield, J. F. *Geochim. Cosmochim. Acta* **1999**, *63*, 1549−1557.
(15) Tang, Z.; Kotov, N. A.; Giersig, M. *Science* **2002**, *297*, 237−240.
(16) Pacholski, C.; Kornowski, A.; Weller H. *Angew. Chem., Int. Ed.* **2002**, *41*, 1188−1191.
(17) Korgel, B. A.; Fitzmaurice, D. *Adv. Mater.* **1998**, *10*, 661−665.
(18) Lu, W.; Gao, P.; Jian, W. B.; Wang, Z. L.; Fang, *J. Am. Chem. Soc.* **2004**, *126*, 14816−14821.

10.1021/ja050107s CCC: $30.25

Table 1. Experimental Conditions Used in Preparation of PbSe Nanocrystals and Nanowires with Different Shape/Morphology[a]

structure	stabilizing agents, solvent	OA:Pb ratio	Pb:Se ratio	injection/growth temperature (°C)	growth time
quasi-spherical nanocrystals	OA-TOP, Ph_2O, or OA-TOP, squalane	4:1	1:3	180/140−160	1−10 min
cubic nanocrystals	OA-TOP, Ph_2O	4:1	1:3	120/110[b]	5−15 min
octahedral nanocrystals	OA-DDA-TOP, Ph_2O	4:1	1:3	230/170	1−2 min
star-shape nanocrystals	OA-HDA-TOP, Ph_2O	4:1	1:3	230/170	2−5 min
undulated nanowires	OA-TOP, Ph_2O	3.15:1	3:1	250/170	1−5 min
zigzag nanowires	OA-HDA-TOP, Ph_2O	3.15:1	3:1	250/180	1−5 min
straight nanowires	OA-TDPA-TOP, Ph_2O	3.15:1	3:1	250/190	30 s−1 min
star-shape branched nanowires	OA-TOP, Ph_2O or OA-HDA-TOP, Ph_2O	3.15:1	3:1	250/170[b]	1−5 min
tapered branched nanowires ("nano-centipedes")	OA-HDA-TOP, octyl ether	3.15:1	3:1	250/170	1−3 min

[a] OA, oleic acid; HDA, hexadecylamine; TOP, trioctylphosphine; Ph_2O, phenyl ether; TDPA, *n*-tetradecylphosphonic acid. [b] Additional injections of Pb:Se precursors.

different nanowire morphologies may be advantageous depending on the applications. Straight nanowires with minimal surface roughness may provide the high carrier mobilities necessary for high-performance FETs.[1] On the other hand, the performance of nanowire-based sensors[5,19] and photovoltaic devices[20] should improve by increasing the wire surface area, that is, highly branched nanowires may best match these applications. The performance of nanowire-based thermoelectric devices[21,22] may substantially benefit from the multiple scattering of acoustic phonons in zigzag and helical nanowires.

The synthesis of high-quality semiconductor nanowires through oriented attachment is demonstrated on the example of lead selenide. PbSe is a direct gap semiconductor with a 0.28 eV band gap in the bulk. It exhibits a large Bohr excitonic radius (46 nm)[23] with nearly identical Bohr radii for the electron (23 nm) and hole (23 nm) and small effective masses for each (<0.1 m_0).[24] Thus in PbSe nanowires, both carriers are strongly confined, allowing their electronic structure to be tuned by changing nanowire diameter. Bulk PbSe exhibits high electron and hole mobilities ($>10^4$ cm^2 V^{-1} s^{-1} at 77 K)[22] and a high thermoelectric figure of merit.[25]

Experimental Section

Chemicals. All manipulations were carried out using standard Schlenk line techniques under dry nitrogen. Tri-*n*-octylphosphine (further referred to as TOP, Strem, 97%), amorphous selenium shots (Aldrich, 99.999%), lead acetate trihydrate (Fisher Scientific Co.), and *n*-tetradecylphosphonic acid (Alfa, 98%) were used as purchased without further purification. Anhydrous methanol, ethanol, 1-butanol, toluene, and tetrachloroethylene were purchased from a variety of sources. To prepare 1.0 M stock solutions of trioctylphosphine selenide (TOPSe), 7.86 g of selenium was dissolved in 100 mL of TOP over 2 h at ∼50 °C.

Synthesis of PbSe Nanowires. An example of synthetic protocol optimized for the preparation of ∼6 nm diameter straight PbSe nanowires follows: 0.76 g of lead acetate trihydrate and 2 mL of oleic acid were dissolved in 10 mL of diphenyl ether. Heating to 150 °C for 30 min under a nitrogen flow forms lead oleate in situ and dries the solution. After cooling to 60 °C, the lead oleate solution was mixed with 4 mL of 0.167 M TOPSe solution in TOP and injected under vigorous stirring into a hot (250 °C) solution containing 0.2 g of *n*-tetradecylphosphonic acid dissolved in 15 mL of diphenyl ether. The injection of stock solution initiated the temperature drop as shown in the reaction temperature profile (Figure S1 of the Supporting Information). After ∼50 s of heating, the reaction mixture was cooled to room temperature using a water bath. The crude solution was mixed with equal volume of hexane, and the nanowires were isolated by centrifugation at 16 000*g* for 5 min. The precipitated nanowires can be redispersed in chloroform forming a stable solution with a tendency of slowly forming birefringent liquid crystalline phases. The reaction conditions for PbSe nanocrystals and nanowires with different morphologies are summarized in Table 1 and Supporting Information.

Synthesis of PbSe Nanorings. The same lead oleate stock solution which has been used for the synthesis of straight PbSe nanowires was injected into the hot (250 °C) solution containing 2 g of hexadecylamine in 15 mL of diphenyl ether. The reaction mixture was kept above 200 °C for 2.5−3 min and then promptly cooled to room temperature. The temperature profile is shown in Figure S1 of the Supporting Information.

Sample Characterization. Powder X-ray diffraction (XRD), transmission electron microscopy (TEM), high-resolution TEM (HRTEM), and energy-dispersive X-ray spectroscopy (EDS) were applied to characterize the size, shape, composition, and structure of synthesized PbSe nanowires. TEM and HRTEM images were collected using Philips CM-12 and EM430 microscopes operating at 120 and 300 kV, respectively. Samples for TEM investigations were prepared by depositing a drop of a dilute nanowire dispersion in chloroform or tetrachloroethylene on a 400 mesh carbon-coated copper grid and allowing the solvent to evaporate at room temperature. Field-effect transistors (FETs) having a channel comprised of PbSe nanowires were fabricated on a heavily n-doped Si wafer, used as a back gate, with a 100 nm thermally grown SiO_2 gate oxide. Ti/Au source and drain electrodes were fabricated by photolithography. PbSe nanowires were aligned across the gap between source and drain electrodes forming a 2 μm semiconducting channel. FET devices were tested using an Agilent 4156B semiconductor parameter analyzer in a nitrogen-filled drybox.

Results and Discussions

PbSe Nanowire Formation. PbSe nanowires shown in Figure 1a are produced by injecting lead oleate and trioctylphosphine selenide mixed with the stabilizing agent, oleic acid, into phenyl ether preheated to 250 °C. The key parameters controlling nanowire formation in this one-step process are the reaction temperature, concentration of the reactants, and concentration and composition of stabilizing agents. Generally, an injection temperature >200 °C and growth temperatures >170 °C are favorable for nanowire formation, while at temperatures <170

(19) Hahm, J.-i.; Lieber, C. M. *Nano Lett.* **2004**, *4*, 51−54.
(20) Huynh, W. U.; Dittmer, J. J.; Alivisatos, A. P. *Science* **2002**, *295*, 2425−2427.
(21) Hicks, L. D.; Dresselhaus, M. S. *Phys. Rev. B* **1993**, *47*, 16631−16634.
(22) Lin, Y.-M.; Dresselhaus, M. S. *Phys. Rev. B* **2003**, *68*, 075304-1−075304-14.
(23) Efros, A. L. *Sov. Phys. Semicond.* **1982**, *16*, 772−775.
(24) Landolt, H. H.; Börnstein, R. *Semiconductors: Physics of Nontetrahedrally Bonded Binary Compounds II*; Springer-Verlag: Berlin, 1983; Vol. III/17f, pp 162−169.
(25) Min, G.; Rowe, D. M. *J. Mater. Sci. Lett.* **1997**, *16*, 1339−1343.

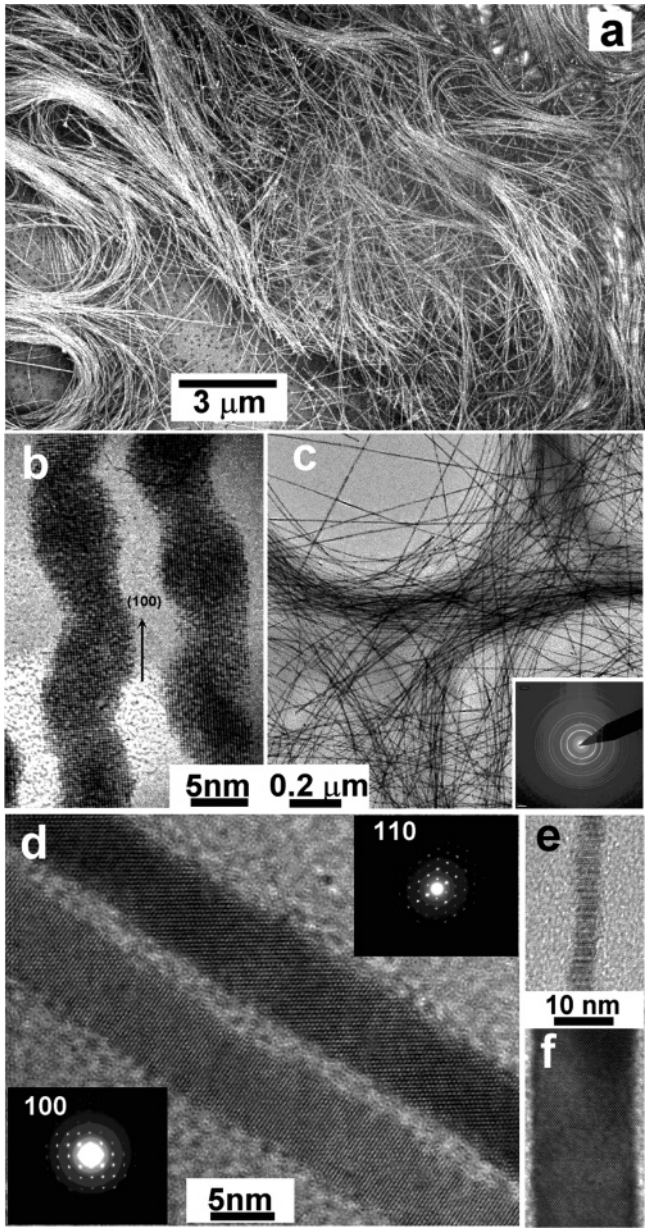

Figure 1. High-resolution (a) SEM and (b) TEM images of PbSe nanowires grown in solution in the presence of oleic acid. (c) Overview and (d−f) high-resolution TEM images of PbSe nanowires formed in the presence of oleic acid and *n*-tetradecylphosphonic acid. Selected area electron diffraction from a film of PbSe nanowires (inset to c) and single nanowires imaged along the (100) and (110) zone axes (insets to d). The diameter of PbSe nanowires can be tuned from (e) ∼4 nm to (f) ∼18 nm.

°C, the same reactants and stabilizing agents form monodisperse nanocrystals.[26] The optimal concentration of oleic acid used for nanowire synthesis is about 80% of that typically employed in the synthesis of PbSe nanocrystals.[26] High Pb:Se reactant ratios increase the yield of the nanowires and the average nanowire length. For example, injecting precursors with a Pb:Se molar ratio of 1:3 at 250 °C yields ∼20% (by volume) of wires with an average length ∼3 μm and 80% particles after 2 min of growth at 170−190 °C. When the Pb:Se ratio is increased to 3:1, the same growth conditions lead to 98% nanowires with an average wire length over 30 μm. Table S1 of the Supporting Information summarizes the effect of reagent concentration and reaction temperature on the yield and length of PbSe nanowires formed in the presence of oleic acid.

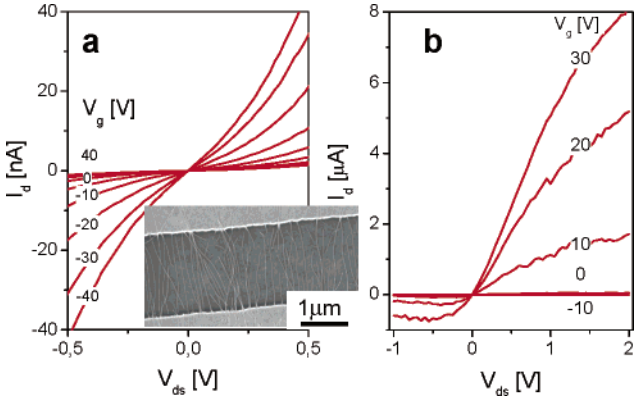

Figure 2. Current−voltage characteristics (drain current, I_d, versus drain voltage, V_{ds}, as a function of gate voltage, V_g) of field-effect transistors made of (a) p- and (b) n-doped PbSe nanowires aligned across 2 μm gaps between source and drain electrodes (inset to a).

When oleic acid is used as the sole stabilizer, PbSe nanowires exhibit significant shape and diameter undulations, as shown in Figure 1b. However, the nanowire shape and morphology can be controlled by introducing cosurfactants into the reaction mixture. For example, long, straight wires with a narrow diameter distribution form in the presence of *n*-tetradecylphosphonic acid (TDPA) (Figure 1c−f). The average length of the nanowires is typically 10−30 μm, while the average diameter can be tuned from ∼3.5 to ∼18 nm with a ∼10% standard deviation by adjusting the temperature profile during growth and controlling the reaction time. Figure 1d shows the HRTEM image of two nanowires with (100) and (110) lattice planes resolved. The insets display the corresponding selected area electron diffraction (SAED) patterns. Surveys of numerous samples using X-ray diffraction (Figure S2 of the Supporting Information), HRTEM, and SAED indicate that the PbSe nanowires are consistently ⟨100⟩ oriented single crystals with the rocksalt structure.

Straight PbSe nanowires can be employed in p-type and n-type FETs, as shown in graphs a and b of Figure 2, respectively, and, therefore, can be used in complementary logic circuits. The type of conductivity is determined by nanowire doping.

One-Dimensional Wires from Zero-Dimensional Nanoparticles. Several indirect observations suggest PbSe nanowires shown in Figure 1 are formed by spontaneous alignment and fusion of PbSe nanoparticles. For example, the formation of PbSe nanorods is observed during the aging of colloidal solutions of PbSe nanocrystals where the excess stabilizing agents have been washed away (Figure 3).

Figure 4a shows the HRTEM images of dimers formed by oriented attachment of PbSe nanocrystals along the ⟨100⟩ axis of the rocksalt lattice. This type of oriented attachment is the most typical for PbSe nanocrystals; however, in the presence of primary amines, attachment along ⟨110⟩ axis is also observed (Figure 4b).

The formation of nanowires via self-assembly of nanoparticles has been studied for several materials.[14−18] Weller et al. reported the formation of ZnO nanorods by oriented attachment of ZnO nanoparticles along the unique axis of its wurtzite crystal

(26) Murray, C. B.; Sun, S.; Gaschler, W.; Doyle, H.; Betley, T. A.; Kagan C. R. *IBM J. Res. Dev.* **2001**, *45*, 47−56.

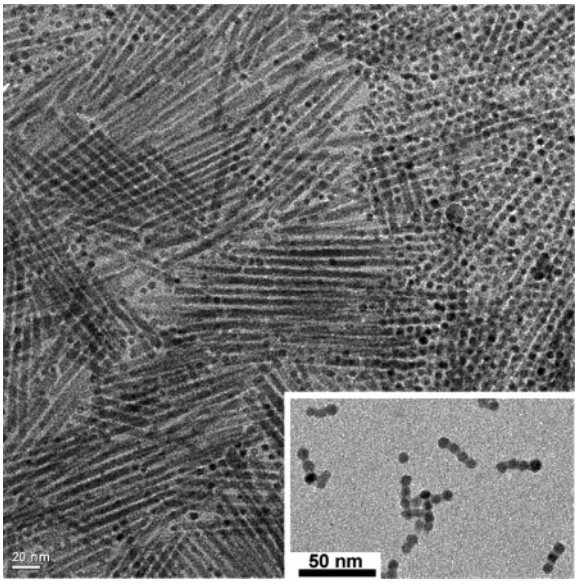

Figure 3. PbSe nanorods formed in a colloidal solution of PbSe nanocrystals washed from an excess of stabilizing agent (oleic acid). Inset shows PbSe "oligomers" formed at early stages in a hot colloidal solution of PbSe nanocrystals.

lattice.[16] The suggested aggregation mechanism is based on the difference in surface structure and reactivity of the (002) and (00$\bar{2}$) faces of the wurtzite lattice. Tang, Kotov, and Giersig demonstrated that wurtzite CdTe nanowires can be formed from zinc blend CdTe nanocrystals after partial removal of the stabilizing agents from the nanocrystals' surfaces.[15] The cubic, zinc blend CdTe nanocrystals formed chainlike aggregates due to induced dipole−dipole interactions at the early stage of wire formation and then slowly recrystallized into hexagonal, wurtzite CdTe nanowires.

The inherent anisotropy of crystal structure or crystal surface reactivity was identified in previous studies as the driving force for the one-dimensional growth. However, 1-D chaining of PbSe rocksalt nanocrystals with their highly symmetric cubic lattice is counterintuitive. Note, to form a 10 μm long nanowire, more than 10^3 individual nanocrystals must assemble and attach along one ⟨100⟩ axis while each PbSe nanocrystal has six equivalent {100} facets. Dipolar interactions seem to be the most probable candidate for the driving force directing PbSe nanocrystals to assemble into chains. However, identifying the origin of a dipole moment for rocksalt PbSe nanocrystals with their centrosymmetric lattice will require additional discussion.

On the Origin of a Dipole Moment in PbSe Nanocrystals. TEM investigations show that the shape of PbSe nanocrystals evolves during growth from quasi-spherical to cubic (Figure 5a). The reconstruction of HRTEM images revealed that relatively small PbSe nanocrystals are terminated by six {100} facets and eight {111} facets. The faster growth of high index {111} facets results in their elimination as the nanocrystal size increases (Figure 5a,b). The {100} facets are formed by both Pb and Se atoms, while the {111} facets must be either Se- or Pb-terminated (Figure 5c). Due to the difference in electronegativities between Pb and Se, {111} facets are polar and their arrangement will determine the distribution of electric charge within the PbSe nanocrystal. The simplest way to maintain PbSe stoichiometry is to terminate four of eight {111} facets by Pb and the other four by Se. The possible arrangements of four

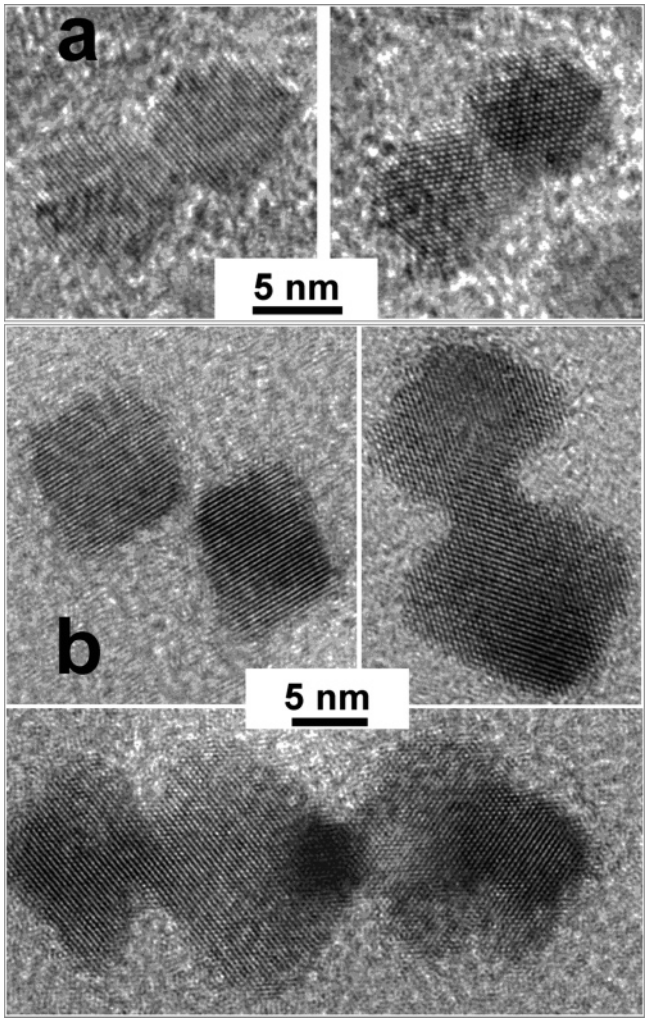

Figure 4. High-resolution TEM images showing oriented attachment of PbSe nanocrystals. (a) Two nanocrystals attached along the ⟨100⟩ crystallographic direction viewed along the (100) and (110) zone axes. (b) Attachment of PbSe nanocrystals along the ⟨110⟩ crystallographic direction (viewed along the (100) zone axis).

Pb-terminated and four Se-terminated {111} facets are shown in Figure 5d. Depending on the mutual arrangement of the {111} facets, the whole nanocrystal can either have central symmetry and thus a zero net dipole moment or it can lack central symmetry and possess a dipole moment along the ⟨100⟩, ⟨110⟩, or ⟨111⟩ axes, respectively (Figure 5d). This, in fact, can explain what drives the oriented attachment of PbSe nanocrystals along various crystallographic axes (Figure 4). Assuming a random distribution of {111} facets, the relative probabilities of a particle having a zero dipole moment or a dipole aligned with the given ⟨*hkl*⟩ crystallographic direction are 0:⟨100⟩:⟨110⟩:⟨111⟩ = 4:15:12:4. The majority of PbSe nanocrystals (~89%) should have nonzero dipole moments! The magnitude of the dipole moment also depends on the distribution of the {111} facets. Thus, the dipole moment along the ⟨100⟩ axis can have two values with the ratio of magnitudes of 2:1 (Figure 5d). Assuming nearly cubic shape and equivalent net charges on all {111} facets, we can roughly estimate the relative magnitudes of dipole moment along different ⟨*hkl*⟩ axes of a PbSe nanocrystal as $\langle 100\rangle_{large}$:$\langle 100\rangle_{small}$:⟨110⟩:⟨111⟩ = $2:1:\sqrt{2}:\sqrt{3}$. The largest dipole moment is predicted along the ⟨100⟩ axis. Summarizing, our model predicts a high fraction of PbSe nanocrystals with permanent

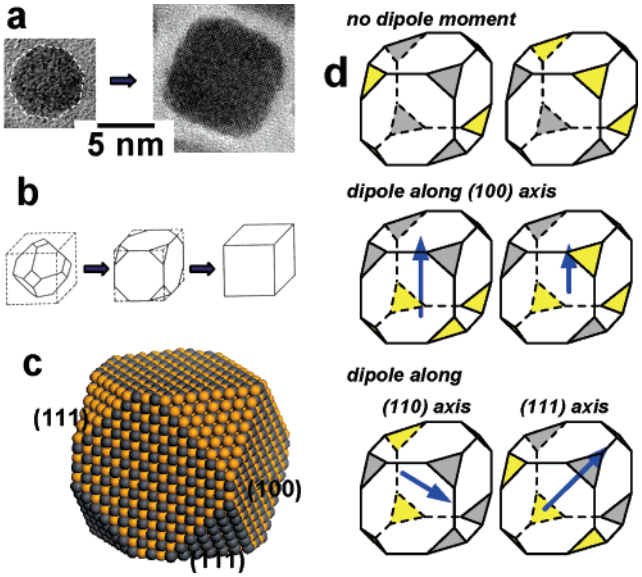

Figure 5. (a) HRTEM images showing the typical evolution of the PbSe nanocrystal shape upon growth, as schematically depicted in (b). (c) Atomic reconstruction of a rocksalt PbSe nanocrystal showing the structural difference between the {100} and {111} facets. (d) Different arrangements of polar {111} facets result in various orientations and magnitudes of the nanocrystal dipole moment (see text for details).

dipole moments. In fact, a permanent dipole moment has been reported for ZnSe nanocrystals with centrosymmetric zinc blend lattice.[27] The highest probability and the largest magnitude of the dipole moment are predicted along the ⟨100⟩ direction. The largest dipolar interactions are predicted for relatively small, "quasi-spherical" nanocrystals, while the larger "nanocubes" should have nearly zero dipole moment. Indeed, relatively small (∼4−5 nm) PbSe nanocrystals can be partially converted into nanowires upon heating in phenyl ether at 150 °C in the presence of 0.22 M oleic acid, while larger (∼10 nm) PbSe nanocubes show no tendency to fuse into nanowires. Long-term heating of nanocube dispersions results in irregular 3-D fusion of the PbSe nanocubes.

When oleic acid and TDPA are utilized as stabilizing agents, we observe only oriented attachment along the ⟨100⟩ axis. Only nanocrystals with dipole moments aligned along the ⟨100⟩ axis can incorporate into the growing nanowires. This is consistent with our observation that the conversion of preformed nanocrystals into nanowires occurs with low yield of nanowires. On the other hand, virtually all nanocrystals assemble into nanowires in the one-pot process, where PbSe nanocrystals nucleate and grow in parallel with the assembly of the nanowires. We explain this by the dynamic character of the dipole in PbSe nanocrystals. The orientation and magnitude of the dipole moment of growing (or dissolving) PbSe nanocrystals can vary in time due to the growth of the Pb- and Se-terminated {111} facets. The nanocrystals are driven to attach to the end of growing nanowires when they have the largest dipole moment along the ⟨100⟩ axis. A similar situation is observed when PbSe nanocrystals slowly etch upon storage in air over a period of weeks. Comparison of TEM images of as-prepared and aged nanocrystals reveals that the efficient assembly of nanorods and nanowires coincides with a decrease of mean nanocrystal size. Although, nanowires formed at room temperature have poor crystallinity, with numerous stacking faults, compared to those formed and annealed at high temperatures.

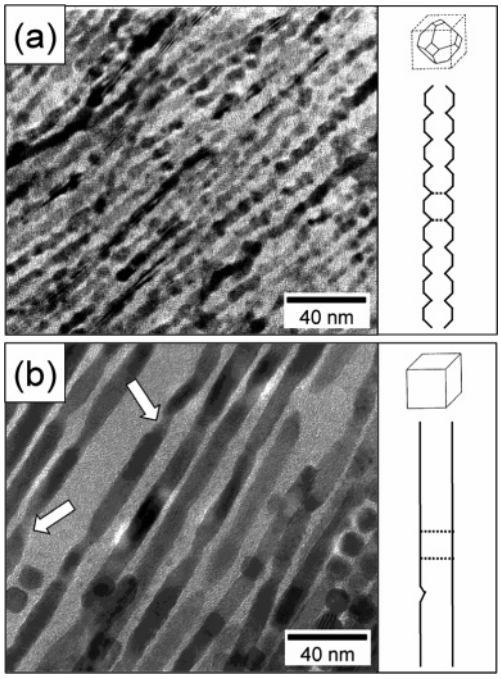

Figure 6. Shape evolution of PbSe nanowires grown for (a) 30 s and (b) 10 min at 170 °C using a molar ratio of Pb:Se precursors of 1:3 and oleic acid as the stabilizing agent. Arrows in (b) point to the (111) face defects. The average wire morphology and the structure of the hypothetical nanocrystal repeat unit are depicted to the right of the TEM images.

In the crude fractions taken during the one-step nanowire synthesis, we observe long (1−30 μm) nanowires and isolated spherical (or cubic) nanocrystals, while dimers and oligomers were very rarely observed. We conclude that the attachment and fusion of the first two PbSe nanocrystals is the rate-limiting step in nanowire formation. Probably, nanowire growth is an avalanche-like process driven by a combination of the increasing polarizability and the scaling of the dipole moment of the growing PbSe nanowire as the number of attached nanocrystals increases.

Controlling PbSe Nanowire Morphology. Once formed, PbSe nanowires can grow radially by consuming the lead and selenium precursors from the surrounding solution. Figure 6 follows the evolution of a single batch of PbSe nanowires grown at 170 °C in the presence of oleic acid and an excess of selenium precursor (Pb:Se = 1:3). The wires evolve from chainlike assemblies, 8 nm in diameter, to straight thicker wires, 12 nm in diameter. The steady growth of the (111) planes results in elimination of the {111} facets, producing straight smooth wires.

The addition of TDPA results in straight and uniform PbSe nanowires (Figure 1c−f). In the presence of TDPA, the reaction mixture remains colorless for ∼10 s after the injection of lead and selenium precursors at 250 °C, indicating that nucleation of the PbSe particles is dramatically delayed. The existence of this "induction period" between injection of the stock solution and nucleation of nanocrystals allows good intermixing of reactants and thermal equilibration of the reaction mixture. This, in turn, improves the nanowire uniformity and narrows diameter distribution. Tighter binding of TDPA molecules to the nanowire surface can decrease the growth rate of both (100) and (111)

(27) Shim, M.; Guyot-Sionnest, P. *J. Chem. Phys.* **1999**, *111*, 6955−6964.

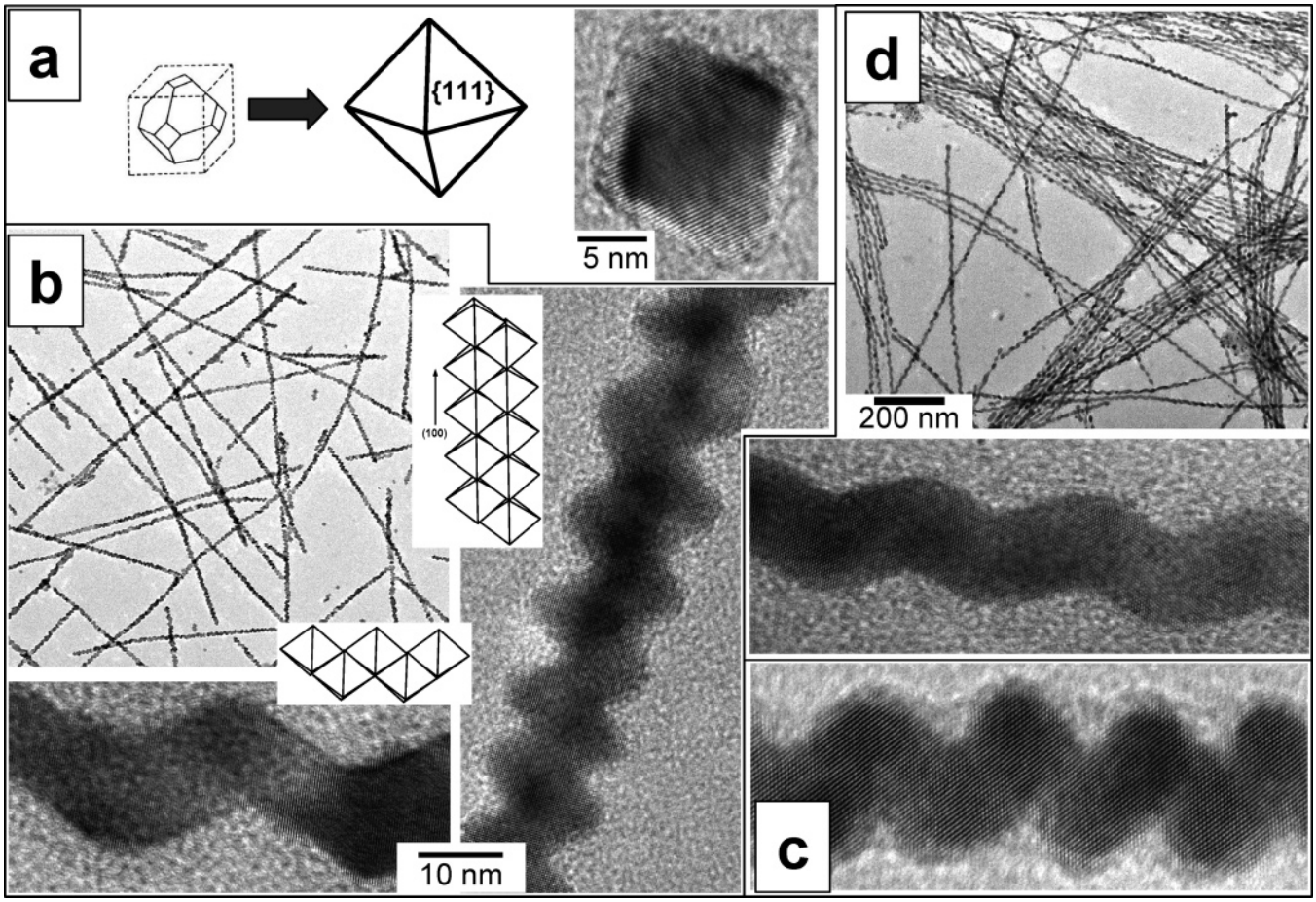

Figure 7. (a) Octahedral PbSe nanocrystals grown in the presence of HDA and oleic acid. (b) TEM and high-resolution TEM images of PbSe zigzag nanowires grown in the presence of HDA. The cartoons show packing of octahedral building blocks to form the nanowires. (c) HRTEM image of single-crystal helical PbSe nanowire grown in oleic acid/HDA/trioctylamine mixture. (d) Helical nanowires formed upon annealing of straight PbSe nanowires, as shown in Figure 1c, in the presence of trioctylamine.

planes, thus allowing more time for diffusion of atoms on nanowire surfaces. To investigate the role of surface diffusion, the rough wires (the wires similar to those shown in Figure 6a) are heated on a heating stage in the TEM. As the temperature is increased up to ~225−230 °C, a significant increase in surface diffusion and annealing is observed. The wires become straighter and displayed well-defined, {100}-faceted sidewalls. Some increase in the diameter of the wires and a corresponding decrease in their length is observed. Reducing the temperature of the stage to ~150 °C quenches the annealing process. We conclude that the {111} facets of rocksalt PbSe have higher energy compared to that of the {100} faces. Monitoring nanowire growth in the presence of surfactants, such as oleic acid and TDPA, also indicates that the {111} facets have higher energy and tend to be eliminated during growth.

The chemical nature of stabilizing agents can significantly affect the surface energy of the different facets of PbSe nanocrystals and nanowires. Addition of long-chain, aliphatic primary amines (e.g., dodecylamine, hexadecylamine (HDA), oleylamine, etc.) to the reaction mixture as cosurfactants induces the formation of octahedral PbSe nanocrystals terminated by eight {111} facets (Figure 7a and Figure S3 of the Supporting Information). To suppress the formation of nanowires, the reaction should be carried out at a low temperature (e.g., injection at 180 °C and growth at 150 °C). The octahedral shape can originate from faster growth of the {100} facets compared to {111} facets, if the latter are selectively blocked by amines.

PbSe nanowires formed by injection at 250 °C and growth at 170 °C in the presence of primary amines exhibit zigzag morphologies, as shown in Figure 7b. The zigzag structure originates from the assembly of octahedral building blocks which share {111} faces. Depending on the mode of octahedron attachment, two kinds of zigzag nanowires are possible, as schematically depicted in Figure 7b. The reaction mixture usually contains both types of nanowires, and the packing of octahedrons can vary along the nanowire. Annealing in octyl ether at 190−200 °C smoothes the zigzag edges. When the nanowires are formed in the presence of HDA as a cosurfactant with oleic acid and when trioctylamine is used as the reaction medium, the formation of single-crystal helical PbSe nanowires has been observed (Figure 7c). Helical PbSe nanowires can also be prepared by the annealing of straight PbSe nanowires, shown in Figure 1c−f at 180−220 °C, in the presence of trioctylamine and oleic acid. The mechanism behind transformation of straight PbSe nanowires into helical ones requires further investigation. Both zigzag and helical PbSe nanowires are potentially interesting for thermoelectric applications offering novel mechanisms of blocking phonon propagation in low-dimensional solids.

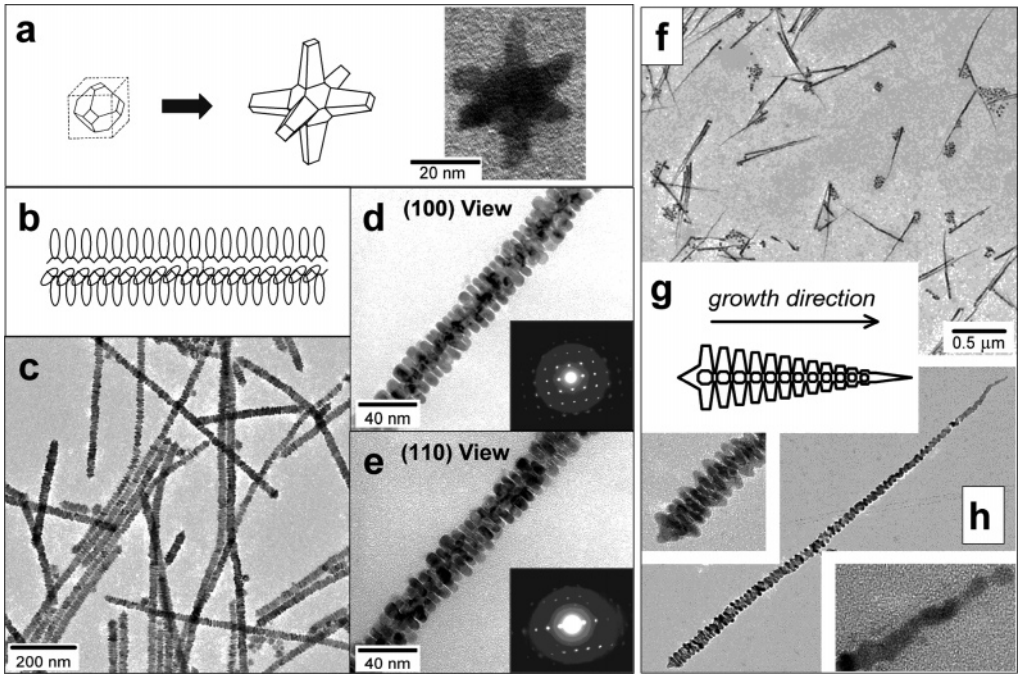

Figure 8. (a) Star-shape PbSe nanocrystals and (b−e) radially branched nanowires. (d) TEM image of the (100) view of the branched nanowire and the corresponding selected area electron diffraction pattern. (e) TEM image of the (110) view of the branched nanowire and the corresponding selected area electron diffraction pattern. The cartoon (b) shows a four-armed branched nanowire. (f and h) Branched nanowires where the length of the sidearms varies along the nanowire, as depicted in cartoon (g).

If growth of the {100} facets is much faster than that of the {111} facets and the particles are allowed to grow for longer time, branched star-shape PbSe nanocrystals are formed due to progressive growth of the {100} facets (Figures 8a and S4 of the Supporting Information). This nanocrystal shape is typical for the reactions employing primary amines, high concentrations of the lead precursor, and phenyl ether as a reaction medium. The growth of nanowires under similar conditions results in radially branched wires (Figure 8b). Figure 8c−e shows the examples of radially branched wires grown with a Pb:Se ratio of 3:1, at 250 °C injection temperature and 170 °C growth temperature. TEM images in Figure 8d,e show projections of the radially branched nanowires along the ⟨100⟩ and ⟨110⟩ axes, respectively. The center-to-center distance between the radial arms is ∼5−6 nm. This is consistent with 5−6 nm particles "polymerizing" by oriented attachment along the ⟨100⟩ axis into a nanowire. The arms grow from the four remaining {100} facets, resulting in radially branched single crystal nanowires (Figure 8b). The long sidearms form if assembly of nanowires from particles is quenched, for example, by fast cooling of the reaction mixture to 170 °C, while the concentrations of lead and selenium precursors are still high. The SAED patterns confirm that the nanowires are single crystals (Figure 8d,e). Note that the presence of sidearms should affect the quantum confinement of the carriers resulting in periodic modulation of the band gap along the nanowire.

The branched nanowires prepared in phenyl ether typically have length up to ∼6 μm, and the sidearms are uniform along the entire length of the nanowire. This indicates that the formation of the central wire and the growth of sidearms are separated in time. Indeed, the oriented attachment and fusion of nanocrystals occurs at temperatures above ∼220 °C on a time scale of several seconds and is completely quenched when temperature drops below ca. 180 °C. On the other hand, the growth of sidearms continues at 170 °C for several minutes.

If the growth rates of the central nanowire and sidearms are comparable, that is, self-assembly of the central nanowire goes in parallel with the growth of the sidearms, the length of sidearms should gradually vary along the nanowire. The longest branches are expected near the origin of the nanowire (Figure 8g). Indeed, using HDA as a cosurfactant and octyl ether as a reaction medium, tapered wires resembling "centipedes" with a clearly distinguishable "head" and "tail" are formed (Figure 8f,h). The length of the sidearms gradually decreases from the head of the centipede toward its tail. Varying the relative rates of central wire assembly and the growth of sidearms allows the length and width of the centipedes to be adjusted.

Formation of tapered wires allows us to suggest that new PbSe nanocrystals can attach only to one end of the growing central wire. To explain this observation, we should assume a significant difference in reactivity of the {001} and {00$\bar{1}$} facets of a growing nanowire with respect to the assembly and oriented attachment. This difference in reactivity is possible if the {001} facet is surrounded with four Se-terminated {111} facets while the {00$\bar{1}$} facet is surrounded with four Pb-terminated {111} facets. Such a surface termination of nanowire ends provides the largest longitudinal dipole moment driving wire assembly. The {001} facet surrounded with four Se-terminated {111} facets can be more reactive than the {00$\bar{1}$} facet surrounded with four Pb-terminated facets capped by bulky oleic acid molecules.

Nanorings. Depending on the orientation of the dipole moment in PbSe nanocrystals and the reaction conditions, we observed oriented attachment of {100} faces (Figure 4a), {110} faces (Figure 4b), and {111} faces (Figure 7b). Controlling the oriented attachment of PbSe nanocrystals along different axes

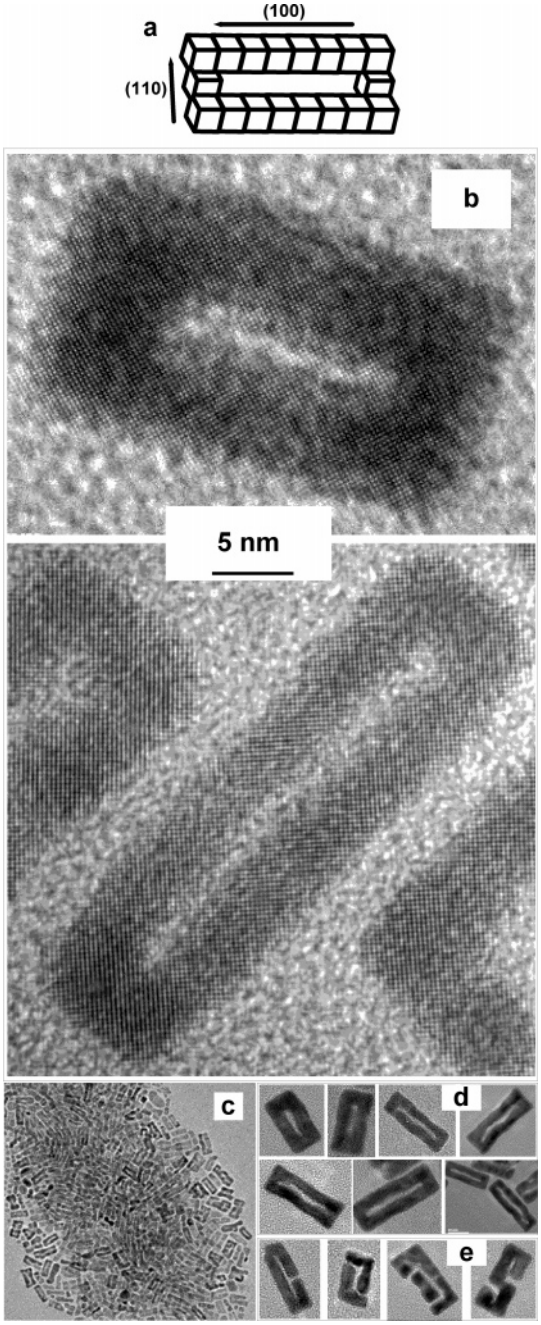

Figure 9. (a) Scheme showing the formation of a nanoring through oriented attachment of PbSe nanocrystals. (b) An overview TEM image of as-synthesized PbSe nanorings. (c and d) TEM images of individual nanorings. (e) The examples showing the early stages of PbSe nanoring formation from the fragments.

would allow formation of nanostructures with complex geometry. Thus, if the reaction is performed in the presence of HDA and at high temperature (injection at 250 °C and growth above 200 °C), we observed formation of smooth, single crystalline rectangular nanorings (Figure 9). The scheme of PbSe nanocrystal assembly to form the nanoring is shown in Figure 9a. The plane of the ring is always the (110) crystallographic plane of PbSe rocksalt lattice (Figure 9b and Figure S5 of the Supporting Information). It is possible to produce nanorings with rather high yield, as seen in Figure 9c,d; however, tight control of the reaction conditions (temperature profile, stirring, and injection rate) is required to achieve reproducibility from run to run. At an early stage in the reaction, we observed incomplete nanorings, as shown in Figure 9e. It appears that the nanorings are assembled not from individual PbSe nanocrystals but from preformed fragments (nanorods) of several fused nanocrystals. The driving force for the assembly of the fragments into nanorings is, probably, dipolar interactions.

Note that both the width and length of rectangular nanorings shown in Figure 9 are smaller than the Bohr excitonic radius in PbSe (46 nm). The electrons and holes in the nanoring should be strongly quantum confined. The ring geometry provides complex boundary conditions for the quantum confined carriers which can result in phenomena not observed in 0-D or 1-D nanostructures. For example, Aharonov−Bohm (AB) oscillations for an exciton in a semiconductor nanoring have recently been predicted.[28] The magnitude of the excitonic AB oscillations should be large for such a small ring and would be observable as oscillations in PL efficiency as the magnitude of a magnetic field applied perpendicular to the plane of the ring is increased. The period of AB oscillations should be ~1.6 T for a 10 nm × 25 nm square ring. The study aimed to understand the behavior of semiconductor nanorings in the strong quantum confinement regime is underway.

Acknowledgment. We thank C. T. Black, C. R. Kagan, and A. Cohen for the assistance with fabrication of field-effect devices, and M. Sviridenko, E. V. Shevchenko, and R. A. Römer for helpful comments and discussions. This work was supported by DARPA through Army Research Office Grant DAAD19-99-1-0001.

Supporting Information Available: Temperature profiles of the reaction mixture during the synthesis of straight PbSe nanowires and nanorings (Figure S1). Additional experimental details and comments to Table 1. Comparison of powder XRD patterns of 10 nm diameter PbSe nanowires and 9.5 nm size PbSe nanocrystals (Figure S2). Volume fraction of nanowires and average nanowire length for different injection temperatures and Pb:Se precursor ratio (Table S1). Overview and high-resolution TEM images of octahedral and star-shape PbSe nanocrystals (Figures S3 and S4). High-resolution TEM images of PbSe nanorings (Figure S5). This material is available free of charge via the Internet at http://pubs.acs.org.

JA050107S

(28) Römer, R. A.; Taikh, M. E. *Phys. Status Solidi B* **2000**, *221*, 535−539.